Plant Physiology®

Plant Physiology, 2024, 196, 1534–1545
https://doi.org/10.1093/plphys/kiae365
Advance access publication 9 July 2024
Research Article

Two calcium sensor-activated kinases function in root hair growth

Xianming Fang,[1,†] Beibei Liu,[1,†] Haiyan Kong,[1] Jingyou Zeng,[1] Yixin Feng,[1] Chengbin Xiao,[1] Qianshuo Shao,[1] Xuemei Huang,[1] Yujun Wu,[2] Aike Bao,[3] Jia Li,[1,4] Sheng Luan,[5,*] and Kai He[1,*]

[1]Ministry of Education Key Laboratory of Cell Activities and Stress Adaptations, School of Life Sciences, Lanzhou University, Lanzhou 730000, China
[2]Academy of Plateau Science and Sustainability, Qinghai Normal University, Xining 810016, China
[3]Key Laboratory of Grassland Livestock Industry Innovation, Ministry of Agriculture and Rural Affairs, State Key Laboratory of Grassland Agro-ecosystems, College of Pastoral Agriculture Science and Technology, Lanzhou University, Lanzhou 730020, China
[4]School of Life Sciences, Guangzhou University, Guangzhou 510006, China
[5]Department of Plant and Microbial Biology, University of California, Berkeley, CA 94720, USA
*Author for correspondence: hekai@lzu.edu.cn (K.H.), sluan@berkeley.edu (S.L.)
[†]These authors contributed equally to this work.
The author responsible for distribution of materials integral to the findings presented in this article in accordance with the policy described in the Instructions for Authors (https://academic.oup.com/plphys/pages/General-Instructions) is: Kai He (hekai@lzu.edu.cn).

Abstract

Plant pollen tubes and root hairs typically polarized tip growth. It is well established that calcium ions (Ca^{2+}) play essential roles in maintaining cell polarity and guiding cell growth orientation. Ca^{2+} signals are encoded by Ca^{2+} channels and transporters and are decoded by a variety of Ca^{2+}-binding proteins often called Ca^{2+} sensors, in which calcineurin B-like protein (CBL) proteins function by interacting with and activating a group of kinases and activate CBL-interacting protein kinases (CIPKs). Some CBL-CIPK complexes, such as CBL2/3-CIPK12/19, act as crucial regulators of pollen tube growth. Whether these calcium decoding components regulate the growth of root hairs, another type of plant cell featuring Ca^{2+}-regulated polarized growth, remains unknown. In this study, we identified *CIPK13* and *CIPK18* as genes specifically expressed in Arabidopsis (*Arabidopsis thaliana*) root hairs. The *cipk13 cipk18* double mutants showed reduced root hair length and lower growth rates. The calcium oscillations at the root hair tip were attenuated in the *cipk13 cipk18* mutants as compared to the wild-type plants. Through yeast 2-hybrid screens, CBL2 and CBL3 were identified as interacting with CIPK13 and CIPK18. *cbl2 cbl3* displayed a shortened root hair phenotype similar to *cipk13 cipk18*. This genetic analysis, together with biochemical assays showing activation of CIPK13/18 by CBL2/3, supported the conclusion that CBL2/3 and CIPK13/18 may work as Ca^{2+}-decoding modules in controlling root hair growth. Thus, the findings that CIPK12/19 and CIPK13/18 function in pollen tube and root hair growth, respectively, illustrate a molecular mechanism in which the same CBLs recruit distinct CIPKs in regulating polarized tip growth in different types of plant cells.

Introduction

In plants, like in many other eukaryotes, calcium ion (Ca^{2+}) serves as a critical second messenger in the signaling pathways that regulate all aspects of growth and development and responses to environmental signals (Kudla et al. 2010; Luan and Wang 2021). The initiation of calcium signals relies on the concentration changes of cellular Ca^{2+}, referring to as calcium signatures that are unique in response to different primary signals such as phytohormones and biotic/abiotic stimuli (McAinsh and Pittman 2009; Tian et al. 2020). It is well accepted that the encoding of Ca^{2+} signals is determined by the Ca^{2+} fluxes mediated by Ca^{2+} channels and transporters localized at plasma membrane (PM) and endomembranes such as tonoplast and endoplasmic reticulum (Hetherington and Brownlee 2004; Dodd et al. 2010). Specific calcium signatures govern downstream signaling events through a Ca^{2+} decoding machinery (Harper et al. 2004; Kudla et al. 2010; Tang et al. 2020). In plants, 4 types of Ca^{2+} decoding proteins are found to directly bind Ca^{2+}, including calmodulin (CaM), CaM-like protein, calcium-dependent protein kinase (CPK), and calcineurin B-like protein (CBL; Edel et al. 2017; Tang et al. 2020; Luan and Wang 2021). The biological information encoded by Ca^{2+} concentration changes is deciphered by the decoding proteins that possess different Ca^{2+} binding affinities and exert a variety of distinct functions.

In plants, isodiametrical growth, anisotropic growth, and tip growth are 3 major types of cell growth (Hussey et al. 2006). Anisotropically expanding cells restrict growth to large and well-defined regions, forming cellular morphologies that grow in different directions. Such cells include root elongation zone cells, as well as leaf pavement cells, among others (Kropf et al. 1998). In tip growth cells, expansion occurs in a small area of the cell surface, resulting in tubular and elongated cells (Kropf et al. 1998; Hussey et al. 2006). Pollen tube and root hair are 2 typical cell types that feature polarized tip growth in plants (Hepler et al. 2001; Cole and Fowler 2006; Qi and Greb 2017). Despite the lack of detailed understanding of the mechanisms underlying polarized cell growth, a number of cellular components are shown to modulate the initiation and maintenance of the polarity in pollen tube and root hair (Rounds and Bezanilla 2013; Pacheco et al. 2023; Zhang et al. 2023). In particular, Ca^{2+} signaling plays crucial roles in polarized growth. A tip-focused Ca^{2+} gradient is found to be crucial for tip growth in both pollen tube and root hair (Bibikova et al. 1997; HoldawayClarke et al. 1997; Cole and Fowler 2006). Ca^{2+} channels

Received October 16, 2023. Accepted May 18, 2024.

are important for encoding Ca^{2+} signals in tip growth. Among them, multiple members in the cyclic nucleotide-gated channel (CNGC) family play essential roles in pollen tube and root hair (Frietsch et al. 2007; Tan et al. 2020). CNGC18 was the first identified CNGC that is required for pollen tube bulging and maintenance of the Ca^{2+} gradient at the cell tip. Loss of function of *CNGC18* results in interrupted pollen tube initiation and cell rapture (Frietsch et al. 2007; Duszyn et al. 2019). CNGC8 and CNGC7 were later found to form a complex with CNGC18 to mediate Ca^{2+} flux in pollen tube and regulate polarized growth by dynamically interacting with CAM2 (Pan et al. 2019). In root hair, CNGC14 functions as a key Ca^{2+} encoding component. Mutation in *CNGC14* leads to disrupted root hair growth when the roots are grown within the agar medium (Zhang et al. 2017). Moreover, simultaneous mutations of *CNGC5*, *CNGC6*, *CNGC9*, and *CNGC14* lead to a dramatic attenuation of cytoplasmic Ca^{2+} oscillations in root hair, which results in shorter and branched root hairs (Brost et al. 2019; Tan et al. 2020).

In animals and fungi, protein phosphatase 2B (PP2B) consists of 2 subunits, calcineurin A (CNA) and calcineurin B (CNB; Sugiura et al. 2002; Creamer 2020). CNA contains a catalytic domain, and CNB associates with Ca^{2+}. The association between CaM and CNA and the binding of Ca^{2+} to CNB EF-hands lead to CNA-CNB dimerization, which activates the activity of PP2B holoenzyme (Creamer 2020). In plants, CBLs interact with and activate CBL-interacting protein kinases (CIPKs; Luan 2009; Tang et al. 2020). The activated CIPK phosphorylates downstream substrates to induce intracellular signal transduction (Weinl and Kudla 2009). Previous research has established the CBL-CIPK network, consisting of 10 CBLs and 26 CIPKs in Arabidopsis (*Arabidopsis thaliana*), as a major signaling paradigm for the regulation of membrane transport across PM and tonoplast (Tang et al. 2020).

In the context of polarized cell growth, earlier studies revealed the essential roles of CBL-CIPK modules in pollen tube growth. Knocking out of either *CIPK12* or *CIPK19* results in defective polarized tip growth in pollen tube (Steinhorst et al. 2015; Zhou et al. 2015). Upstream of CIPK12, CBL2/3 may be the Ca^{2+} sensors initiating the regulatory process at the vacuolar site (Steinhorst et al. 2015). However, it remains unknown whether similar CBL-CIPK modules are adopted in controlling root hair growth.

In this study, we show that *CIPK13* and *CIPK18*, the homologs of *CIPK12* and *CIPK19*, play critical roles in regulating the polarized growth in root hair. Simultaneous mutations in *CIPK13* and *CIPK18* cause partially impaired root hair growth. The tonoplast-localized Ca^{2+} sensors, CBL2 and CBL3, interact with and activate CIPK13 and CIPK18. Furthermore, the genetic results indicate *CIPK12* and *CIPK19* specifically function in pollen tube while *CIPK13* and *CIPK18* exclusively act in root hair. Thus, we demonstrate that the *CIPK* subclades containing *CIPK12*, *CIPK13*, *CIPK18*, and *CIPK19* likely serve as essential Ca^{2+} decoding regulators in modulating polarized cell tip growth, and that different CIPK-CBL complexes fulfill their roles either in pollen tube or in root hair.

Results

CIPK12/19, not *CIPK13/18*, are involved in regulating pollen tube growth

Previous studies revealed that both *CIPK12* and *CIPK19* are involved in the polarized cell growth in pollen tube (Steinhorst et al. 2015; Zhou et al. 2015). When *CIPK12* or *CIPK19* is knocked out, the mutant plants show shortened pollen tube length and lower growth rates compared to wild-type (WT) plants. However, neither *cipk12* nor *cipk19* exhibits substantial morphological differences to WT at all developmental stages, and its fertility is totally normal (Steinhorst et al. 2015; Zhou et al. 2015). Given that *cipk12* and *cipk19* single mutants only showed slightly impaired pollen tube growth, we set to investigate whether *CIPK12* and *CIPK19* are functionally redundant and/or additional *CIPKs* contribute to pollen tube growth by examining higher-order mutant plants. The *cipk12-3* and *cipk19-1* single mutant plants were isolated, and multiple mutants were generated by genetic crosses (Supplementary Fig. S1A). RT-PCR was used to confirm that all *cipk* T-DNA insertion lines tested in this study were null mutants (Supplementary Fig. S1B and Table S1). Consistent with earlier results, *cipk12-3* and *cipk19-1* single mutants showed slightly shortened pollen tube when germinated in vitro (Supplementary Fig. S2). However, *cipk12-3 cipk19-1* double mutant exhibited similar pollen tube phenotype as the single mutants, suggesting *CIPK12* and *CIPK19* are not functioning synergistically (Supplementary Fig. S2). We noticed that CIPK12 and CIPK19 belong to a subclade in the CIPK family, which contains 4 members including CIPK12, CIPK13, CIPK18, and CIPK19 (Supplementary Fig. S3A). We next analyzed the expression patterns of the 4 *CIPK* genes by using transgenic plants containing a GUS reporter. The GUS staining patterns indicated that *CIPK12*, *CIPK13*, *CIPK18*, and *CIPK19* were expressed in roots and floral organs. In leaves, expression of *CIPK12*, but not *CIPK13*, *CIPK18*, or *CIPK19*, was detected at a significant level (Supplementary Fig. S4).

We next conducted genetic analysis by obtaining *cipk13* and *cipk18* single mutants and *cipk12 cipk19 cipk13 cipk18* quadruple mutant. Compared to *cipk12-3 cipk19-1* double mutant, *cipk12-2 cipk19-1 cipk13-2 cipk18-1* quadruple mutant displayed similar defect in pollen tube growth, indicating that *CIPK13* and *CIPK18* are not likely involved in pollen tube growth (Supplementary Fig. S3, B to D). To further understand the mechanisms of *CIPK*-regulated pollen tube growth, we examined the expression of these 4 *CIPKs* in pollen tube in details. By analyzing the transgenic plants harboring *proCIPK::nls-YFP*, we found *CIPK12* and *CIPK19* were clearly expressed in mature pollens and pollen tubes (Supplementary Fig. S5), consistent with previous reports (Steinhorst et al. 2015; Zhou et al. 2015), whereas the expression of *CIPK13* and *CIPK18* was not clearly detected in pollens or pollen tubes (Supplementary Fig. S5). These results thus demonstrated that only *CIPK12* and *CIPK19*, but not *CIPK13* and *CIPK18*, contribute to pollen tube growth.

CIPK13 and *CIPK18* are expressed in root hairs

Interestingly, we noticed that *CIPK13* and *CIPK18* are highly expressed in root hair, another cell type showing polarized cell growth (Fig. 1A). By contrast, *CIPK12* and *CIPK19* showed no or very weak expression in root hair cells (Fig. 1A). To verify the expression of these *CIPKs*, the root hairs of the transgenic plants harboring *proCIPK::nls-YFP* were analyzed. The promoters of *CIPK13/18* were found to be active in root hair cells. In addition to pollen tubes, the YFP signals in *proCIPK12/19::nls-YFP* plants were detected in vascular tissues, but not in root hairs (Fig. 1B). Furthermore, we examined the subcellular location of CIPK13/18 and found that both CIPK13 and CIPK18 proteins mainly located in the cytoplasm (Fig. 1C).

The *cipk13 cipk18* mutants show reduced root hair length and lower growth rate

We next examined the root hair phenotype of *cipk13* and *cipk18* single/double mutants. When grown vertically on the surface of agar medium, all plants showed no difference regarding root hair morphology (Supplementary Fig. S6). To mimic the surrounding environment of root growth, all plant lines were planted on the

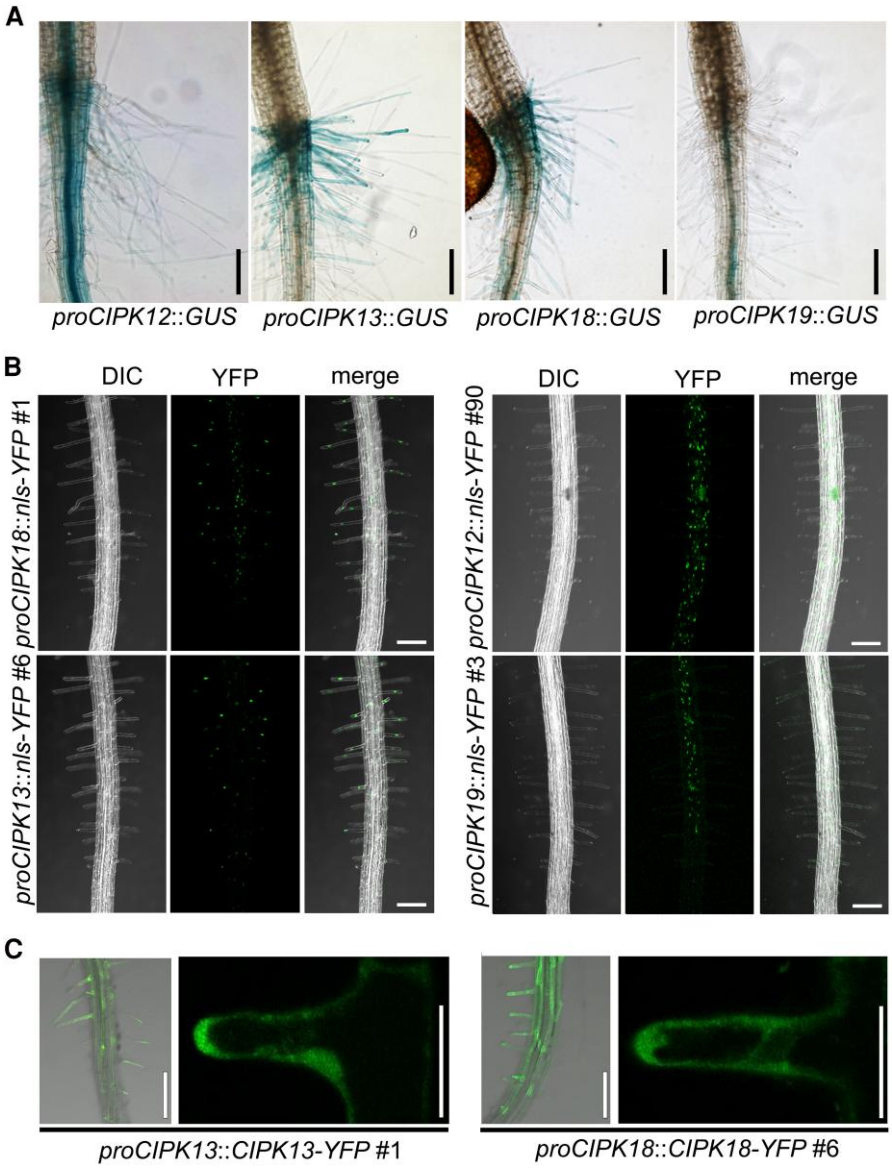

Figure 1. *CIPK13* and *CIPK18* are expressed in root hair cells. **A)** GUS staining of root hair cells of 4-d-old plants. Bars = 0.2 mm. **B)** *Promoter*::*nls-YFP* transgenic plants for *CIPK12*, *CIPK13*, *CIPK18*, and *CIPK19* were analyzed. The fluorescence signal of the root hair region of 4-d-old seedlings was observed. Bars = 0.2 mm. **C)** *Promoter*::*CDS-YFP* transgenic plants for *CIPK13* and *CIPK18* were analyzed. The fluorescence signal of the root hair region of 4-d-old seedlings was observed. Bars = 0.2 mm (left) and 50 μm (right).

top of agar medium and the roots of the seedlings were grown within the medium. Neither *cipk13-2* nor *cipk18-1* single mutant displayed obvious root hair defects. The *cipk13-2 cipk18-1* double mutant, however, showed obvious shortened root hairs (Fig. 2A). To verify the root hair phenotype, an additional set of double mutants, *cipk13-c1 cipk18-c1*, was constructed by using CRISPR/Cas9 (Supplementary Fig. S7). *cipk13-c1 cipk18-c1* exhibited a defective root hair phenotype similar to *cipk13-2 cipk18-1* (Supplementary Fig. S6). Next, *cipk13 cipk18* was complemented with *CIPK13* or *CIPK18* genomic sequence (Supplementary Fig. S8, A and B). Either *CIPK13* or *CIPK18* was able to fully rescue the root hair phenotype of *cipk13-2 cipk18-1* (Fig. 2, A to C).

By analyzing root hair cells that bugle at the same stage in *cipk13 cipk18* and WT, we found that the root hair elongation of *cipk13 cipk18* was remarkably slower than that of WT. At 60 min, the length of root hairs was about 50 μm in *cipk13 cipk18* but around 60 μm in WT (Fig. 2, D and E).

We next examined whether *CIPK12* and *CIPK19* are involved in root hair growth. Compared to *cipk13-2 cipk18-1*, no obvious difference was detected in the root hair of *cipk12-3 cipk13-2 cipk18-1 cipk19-1*, suggesting *CIPK12* and *CIPK19* are not engaged in root hair growth (Supplementary Fig. S9).

The calcium oscillations are attenuated in *cipk13 cipk18*

CIPKs act as Ca^{2+} sensor-activated components in Ca^{2+} decoding. We next analyzed the Ca^{2+} signals in 2 sets of *cipk13 cipk18* lines. The Col-0 plants harboring *GCaMP6s*, encoding a Ca^{2+} indicator, were crossed to *cipk13 cipk18*. The higher the Ca^{2+} concentration presented, the stronger the fluorescence detected. We examined the concentration changes of Ca^{2+} at the cross-sections of Col-0 and *cipk13 cipk18* at a time course of 90 s. We found the Ca^{2+} oscillations were significantly weaker in *cipk13 cipk18* compared to WT (Fig. 3A; Supplementary

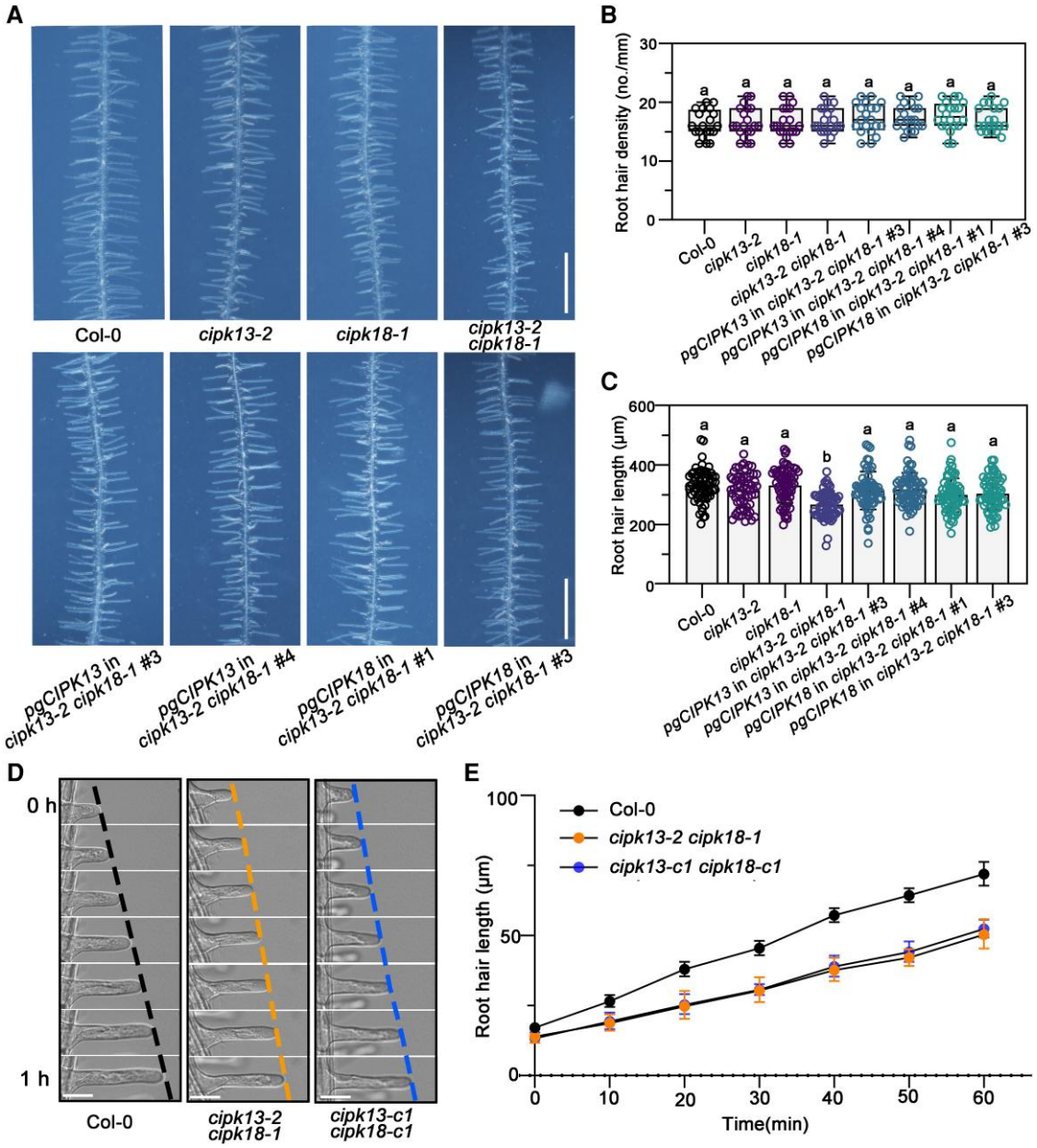

Figure 2. *CIPK13* and *CIPK18* are required for root hair growth. **A)** Representative images of 4-d-old seedlings of Col-0, *cipk13-2*, *cipk18-1*, *cipk13-2 cipk18-1*, and complemented (COM) lines. The roots are grown within the agar medium. Bars = 0.5 mm. **B and C)** Statistical analysis of root hair densities and root hair lengths for the plant lines presented in **A)**. For root hair densities, different letters represent significant differences ($P < 0.05$) determined by 1-way ANOVA with Tukey's multiple comparison test (center line, median; box limits, upper and lower quartiles; whiskers, minimal to maximal value; $n > 12$ plants). Root hair lengths are presented as mean ± SD (data were collected from more than 100 root hairs). The results were analyzed with 1-way ANOVA and Tukey's multiple comparison test ($P < 0.05$, marked with different characters). **D)** Growth dynamics of individual Col-0 and *cipk13 cipk18* root hairs. The consecutive frames of growing root hairs for a period of 60 min. Photos were taken every 10 min. The dotted lines represent the root hair growth at same times. Bars = 20 μm. **E)** Statistical analysis of root hair lengths per unit time. Root hair lengths are presented as mean ± SD (data were collected from 10 root hairs).

Video S1). The statistical results indicated that the maximum mean fluorescence intensity can reach around 200 AU in Col-0 but only about 175 AU in *cipk13 cipk18* (Fig. 3B). It suggested Ca^{2+} coding processes are impaired when *CIPK13* and *CIPK18* are absent.

We next analyzed whether additionally supplied Ca^{2+} or EGTA affects the phenotype of *cipk13 cipk18*. When the plants were grown on the surface of the medium, the treatment of Ca^{2+} or EGTA had no effect on the root hair density or root hair length of *cipk13 cipk18* and Col-0 (Supplementary Fig. S10, A to C). When grown within the agar medium, no root density difference was observed between *cipk13 cipk18* and Col-0 upon EGTA or Ca^{2+} supplement (Supplementary Fig. S10, D and E). However, EGTA, but not Ca^{2+}, appeared to abolish the phenotypic difference between *cipk13 cipk18* and Col-0 (Supplementary Fig. S10, D and F), indicating Ca^{2+} signal is critical in *CIPK13/18*-mediated root hair regulation.

CBL1/2/3/9 interact with CIPK13/18

CIPKs are not directly activated by Ca^{2+}. Instead, Ca^{2+} binds to CBLs that subsequently interact with and activate CIPKs.

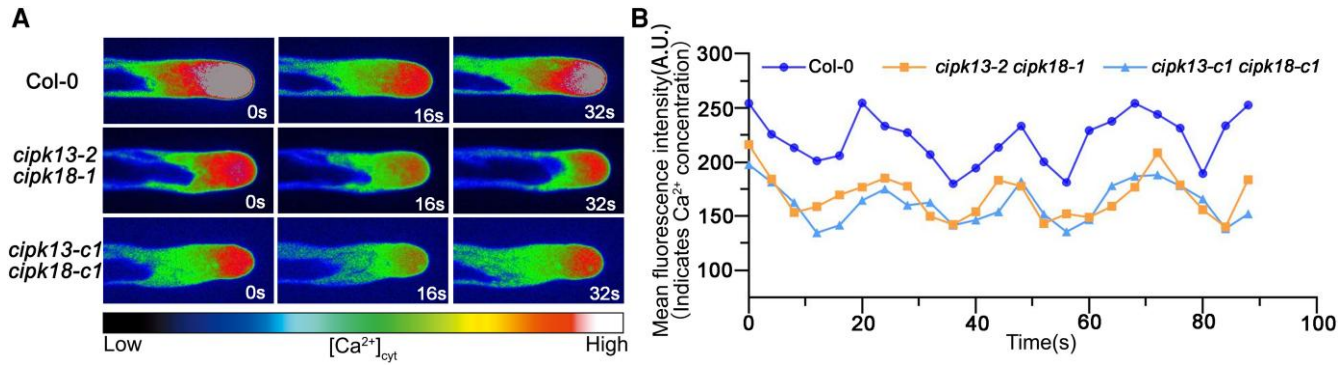

Figure 3. Calcium oscillations are attenuated in *cipk13 cipk18* root hair. **A)** Root hairs of Col-0 and *cipk13 cipk18* expressing the Ca^{2+} sensor *GCaMP6s* were imaged every 4 s. Numbers represent time in seconds. **B)** Quantitative analysis of cytosolic Ca^{2+} oscillations in growing root hairs of Col-0 and *cipk13 cipk18*. These experiments were repeated at least 4 times with similar results.

To seek for the CBLs that function as the activators of CIPK13 and CIPK18, a yeast 2-hybrid screen was performed. All 10 *CBLs* were cloned into AD vector, and *CIPK13/18* were recombined into BD vector. On synthetically defined (SD) media lacking Leu (L), Trp (W), and His (H), CIPK13 interacted with CBL2/3 while CIPK18 broadly associated with most of the CBLs. On SD media lacking Leu (L), Trp (W), Ade (A), and His (H), CIPK18 was shown to strongly interact with CBL1/2/3/9 and CIPK13 only obviously interacted with CBL2 (Fig. 4A).

CBL2/3 function in CIPK13/18-mediated root hair regulation

CBL1 and CBL9 are usually functionally redundant while CBL2 and CBL3 often show overlapping functions. CBL1/9 locate at PM and recruit the interacting CIPKs to proximity to the cell surface. CBL2/3 are tonoplast localized and contribute to vacuole-related modulations (Tang et al. 2012). Since CIPK13/18 likely interact with CBL1/9 and CBL2/3, it remained to determine which CBL pairs are involved in the root hair regulation. To this end, *cbl1-1 cbl9-1* and *cbl2-2 cbl3-2* double mutants were obtained. The double mutants were cultured on the medium with the roots grown within the agar. Similar to *cipk13-2 cipk18-1*, *cbl2-2 cbl3-2* exhibited shortened root hair phenotype. The root hair of *cbl1-1 cbl9-1* was identical to that of Col-0 (Fig. 5). The defective root hair phenotype of *cbl2-2 cbl3-2* was verified by complementation assays. Introduction of *CBL3* fully recued the shortened root hairs in *cbl2-2 cbl2-3* (Supplementary Figs. S8, E and F, and S11, F to H). Moreover, the second set of *cbl2 cbl3* double mull mutant, *cbl2-c1 cbl3-c1*, was generated by CRISPR/Cas9 (Supplementary Fig. S11A). *cbl2-c1 cbl3-c1* displayed arrested growth and earlier senescence similar to *cbl2-2 cbl3-2* around 30 d (Supplementary Fig. S11B). Likewise, *cbl2-c1 cbl3-c1* exhibited shortened root hairs identical to *cbl2-2 cbl3-2* when grown in the agar medium (Supplementary Fig. S11, C to E). These results suggested that CBL2/3 act as the Ca^{2+} sensors that activate CIPK13/18 in regulating root hair growth.

The CBL2/3-CIPK13/18 interactions were further verified by bimolecular fluorescence complementation (BiFC) in *Nicotiana benthamiana*. Both CBL2 and CBL3 were found to interact with CIPK13 and CIPK18 (Fig. 4B). As a control, CBL10 failed to interact with CIPK13 or CIPK18 (Fig. 4B). Of note, the detailed analysis of BiFC results demonstrated the interactions of CIPK13/18 and CBL2/3 occurred at tonoplast (Fig. 4B). The association between CIPK18 and CBL3 was next examined by using coimmunoprecipitation (Co-IP) in *N. benthamiana*. The results confirmed that CIPK18 and CBL3 interacted with each other in planta (Fig. 4C). In summary, these results suggested CBL2/3 are the candidates that function upstream of CIPK13/18.

The genetic analyses of *CIPK13/18* and *CBL2/3*

We next investigated the genetic interactions between *CIPK13/18* and *CBL2/3*. Compared to *cipk13-2 cipk18-1* or *cbl2-2 cbl3-2* double mutant, the quadruple mutant plants showed no addictive root hair defect (Fig. 6, A to C). When overexpressed, *CIPK13* had no effect on the root hair growth of *cbl2-2 cbl3-2* (Fig. 6, D to G; Supplementary Fig. S8G). Likewise, the overexpression of *CBL2/3* failed to alter the root hair phonotype of *cipk13-2 cipk18-1* (Fig. 6, H to K; Supplementary Fig. S8D). Furthermore, we constructed *cipk13-2 cipk18-1 cbl2-2 cbl3-2* quadruple mutant (Supplementary Fig. S8C). The results thus demonstrated that *CIPK13/18* and *CBL2/3* are genetically required for each other in terms of regulating root hair growth.

CIPK13/18 are activated by CBL2/3

The phenotypic analysis of *cbl2-2 cbl3-2* supported a notion that CBL2/3-CIPK13/18 act as functional units in modulating root hair growth. CBLs serve as crucial Ca^{2+} sensors that decipher Ca^{2+} oscillations and transduce Ca^{2+} signals into physiological responses via promoting the kinase activities of CIPKs. We thus investigated whether CBL2/3 are able to activate CIPK13/18. The autophosphorylation of CIPK13/18 was examined by using an anti-pT/Y antibody. The presence of CBL2/3 significantly enhanced the phosphorylation levels of CIPK13/18 (Fig. 7, A and B). By contrast, the phosphorylation of CIPK13/18 was not affected by GST (Supplementary Fig. S12). The CIPK transphosphorylation ability was next examined. Our previous screen identified the loop domain of a channel protein, OSCA2.3, interacted with CIPK18 (Supplementary Fig. S13). Although the biological significance of this interaction is still unclear, the OSCA2.3 loop can serve as a substrate to test the kinase activity of CIPK18. By using a kinase assay based on [γ-^{32}p]-ATP, we found CBL3 clearly promoted the autophosphorylation of CIPK18 via autoradiography, similar to western blot results. Furthermore, OSCA2.3 loop was phosphorylated by CIPK18 when CBL3 was present (Fig. 7C). Of note, CBL3 was also strongly phosphorylated by CIPK18 (Fig. 7C). Taken together, our results indicated CBL2/3 are capable of activating CIPK13/18 regarding both autophosphorylation and transphosphorylation.

Discussion

The central roles of calcium in modulating polarized cell growth have been well documented. In this study, we show CBL-activated

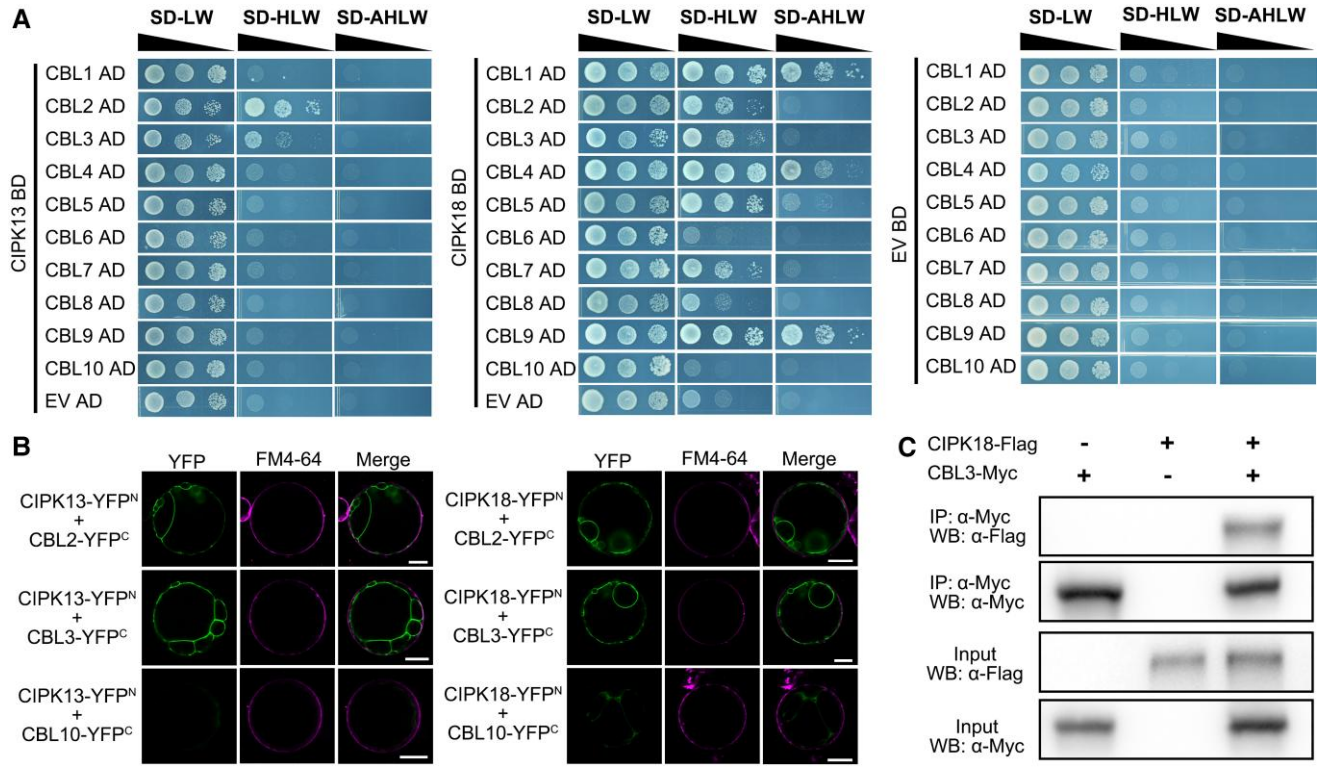

Figure 4. CBLs interact with CIPK13 and CIPK18. **A)** The interactions between CIPK13/18 and CBLs shown by yeast 2-hybrid. Serial decimal dilutions of yeast cells were grown on SD medium without Leu and Trp (-LW) and on SD medium without His, Leu, Trp, or Ade (-HLW)/(-AHLW). Photos were taken after 3 to 5 d of growth on the indicated medium. **B)** The interactions between CIPK13/18 and CBL2/3 shown by BiFC in *N. benthamiana* protoplasts. CBL10 was used as a negative control. Pairs of split-YFP constructs were transiently coexpressed in *N. benthamiana* protoplasts. YFP and FM4-64 fluorescence signal was detected using a confocal microscopy after 48 h of infiltration. Bars = 20 μm **C)** The interaction between CIPK18 and CBL3 shown by Co-IP in *N. benthamiana*. Proteins immunoprecipitated with an α-Myc antibody were analyzed with an α-Flag or α-Myc antibody. These experiments were repeated at least 3 times with similar results.

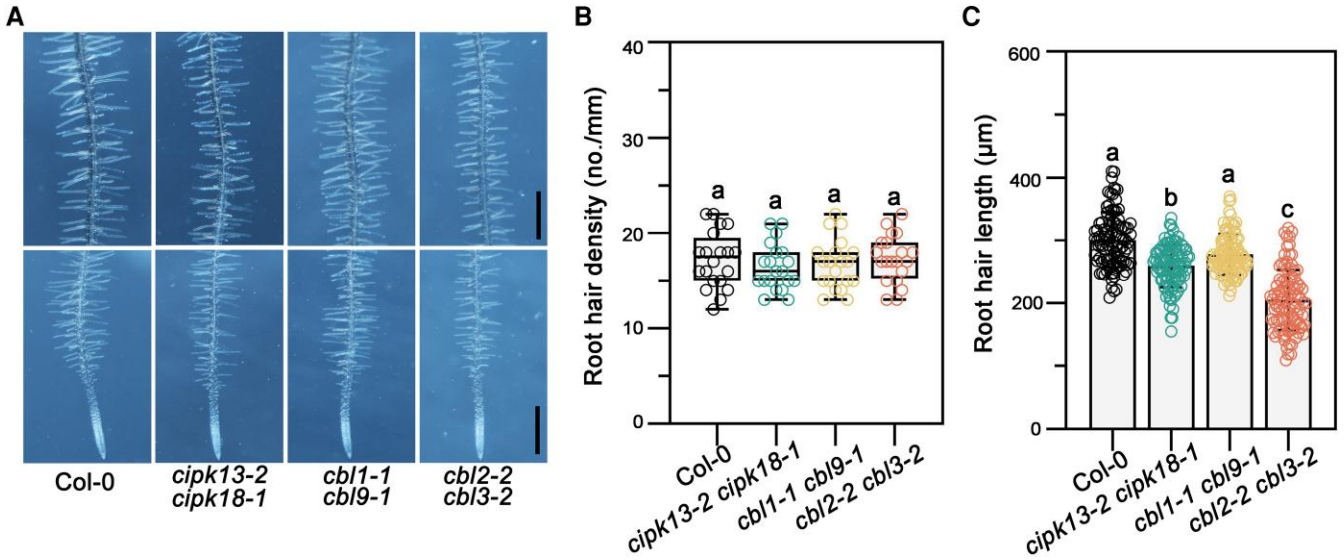

Figure 5. *cbl2 cbl3* shows defective root hair growth similar to *cipk 13 cipk18*. **A)** Representative images of 4-d-old seedlings of Col-0, *cipk13-2 cipk18-1*, *cbl1-1 cbl9-1*, and *cbl2-2 cbl3-2* grown in the medium. Bars = 0.5 mm. **B and C)** Statistical analysis of root hair densities and root hair lengths of the plant lines presented in **A)**. For root hair densities, different letters represent significant differences ($P < 0.05$) determined by 1-way ANOVA with Tukey's multiple comparison test (center line, median; box limits, upper and lower quartiles; whiskers, minimal to maximal value; $n > 12$ plants). Root hair lengths are presented as mean ± SD (data were collected from more than 100 root hairs). The results were analyzed with 1-way ANOVA and Tukey's multiple comparison test ($P < 0.05$, marked with different characters).

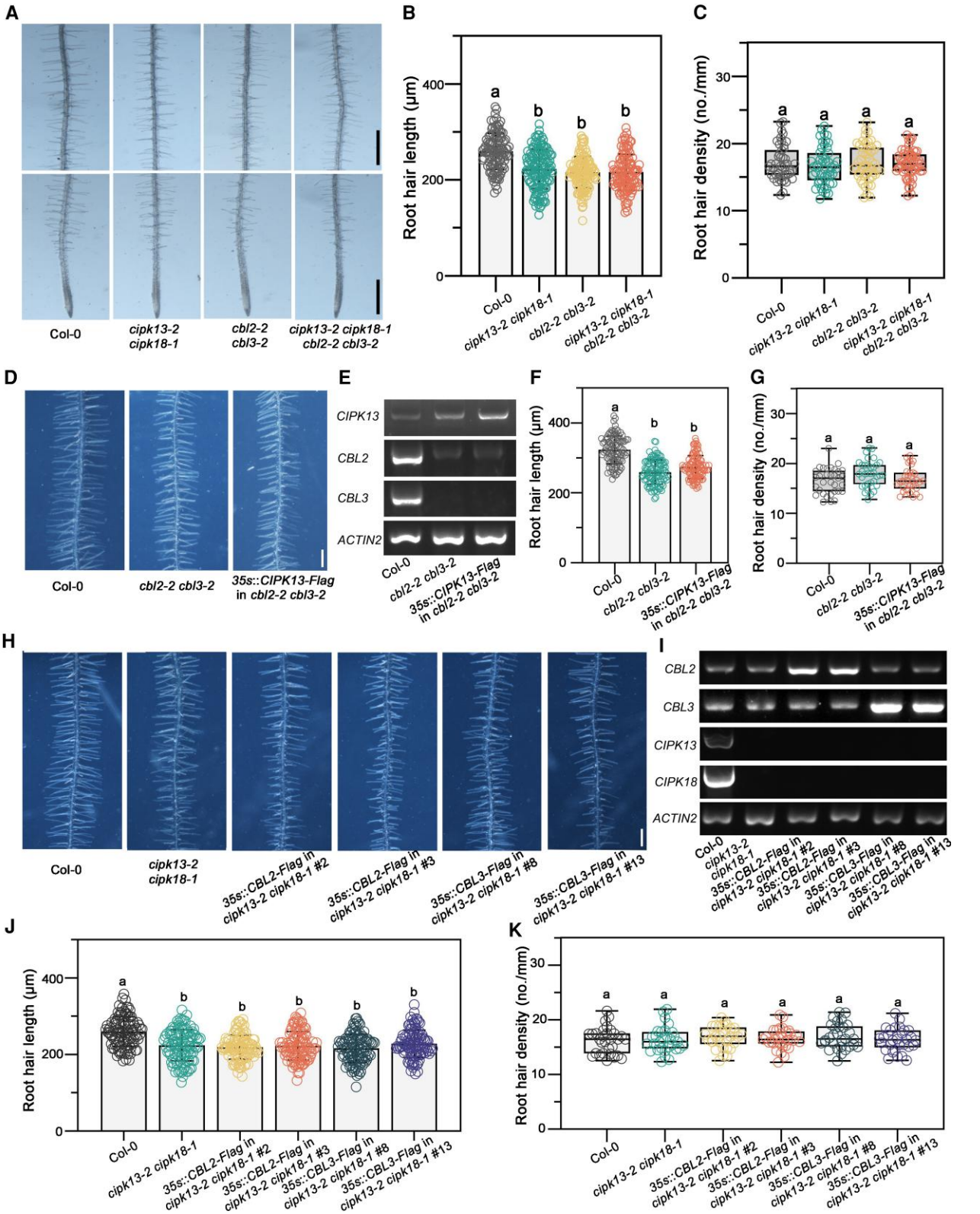

Figure 6. Genetic analyses of *CIPK13/18* and *CBL2/3*. **A)** Representative images of 4-d-old seedlings of Col-0, *cipk13-2 cipk18-1*, *cbl2-2 cbl3-2*, and *cipk13-2 cipk18-1 cbl2-2 cbl3-2* grown in the medium. Bars = 0.5 mm. **B and C)** Statistical analysis of root hair lengths and root hair densities of the plant lines presented in **A)**. **D)** Representative images of 4-d-old seedlings of Col-0, *cbl2-2 cbl3-2*, and *CIPK13* overexpression lines in *cbl2-2 cbl3-2* grown in the medium. Bar = 0.2 mm. **E)** RT-PCR identification of mutants in **D)**. **F and G)** Statistical analysis of root hair lengths and root hair densities of the plant lines presented in **D)**. **H)** Representative images of 4-d-old seedlings of Col-0, *cipk13-2 cipk18-1*, and *CBL2/3* overexpression lines in *cipk13-2 cipk18-1* grown in the medium. Bar = 0.2 mm. **I)** RT-PCR identification of the mutant plants in **H)**. **J and K)** Statistical analysis of root hair lengths and root hair densities of the plant lines presented in **H)**. For root hair densities, different letters represent significant differences ($P < 0.05$) determined by 1-way ANOVA with Tukey's multiple comparison test (center line, median; box limits, upper and lower quartiles; whiskers, minimal to maximal value; $n > 12$ plants). Root hair lengths are presented as mean ± SD (data were collected from more than 50 root hairs). The results were analyzed with 1-way ANOVA and Tukey's multiple comparison test ($P < 0.05$, marked with different characters).

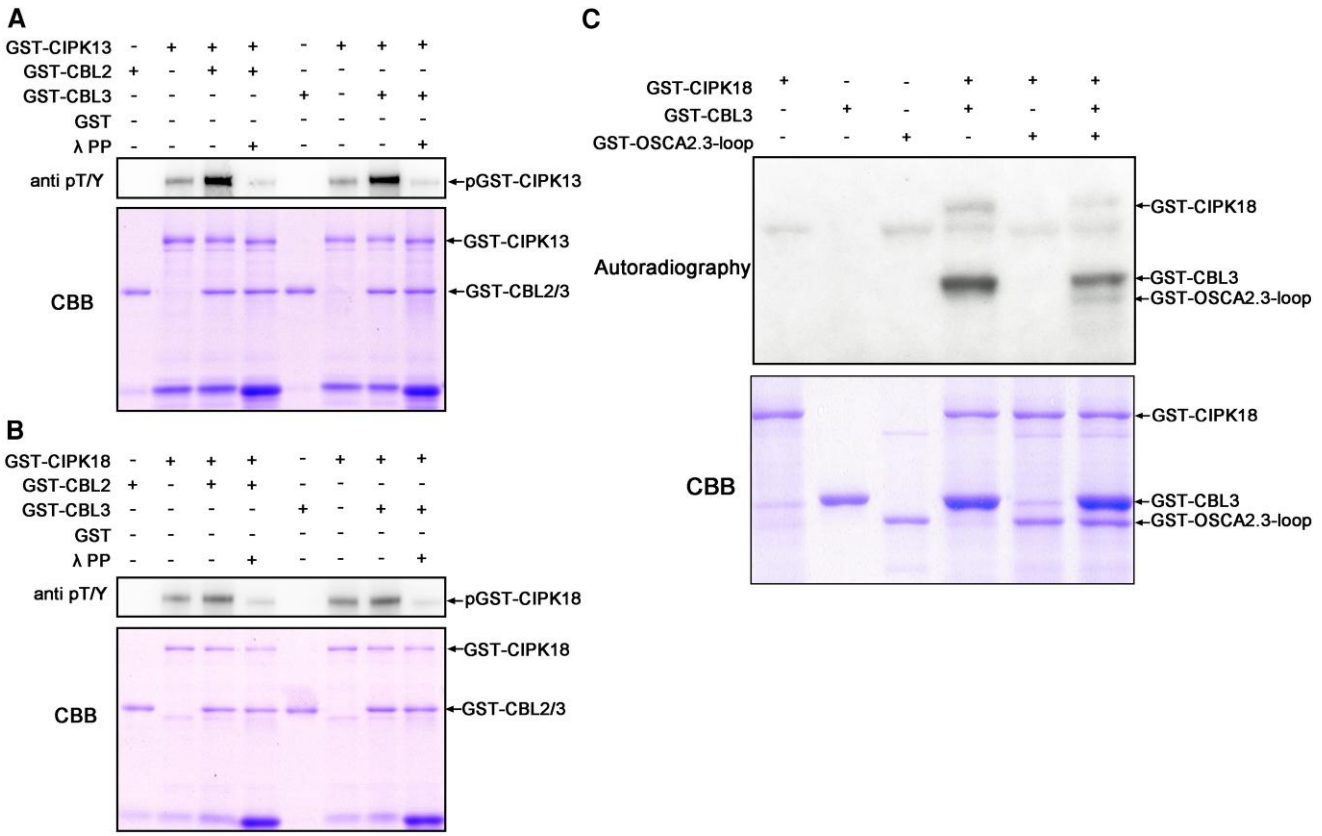

Figure 7. CBL2/3 activate CIPK13/18. **A)** The autophosphorylation levels of CIPK13 are activated by CBL2 or CBL3. **B)** The autophosphorylation levels of CIPK18 are activated by CBL2 or CBL3. CIPKs or CBLs fused with glutathione S-transferase (GST) tag were purified. Phosphorylated proteins were separated by SDS–PAGE gels and detected by a phospho-threonine/tyrosine antibody (upper panels). Total proteins were Coomassie Brilliant Blue (CBB) stained in SDS–PAGE gels (bottom panels). **C)** The transphosphorylation ability of CIPK18 is activated by CBL3. Phosphorylated proteins were detected by in vitro kinase assay based on [γ-^{32}P]-ATP.

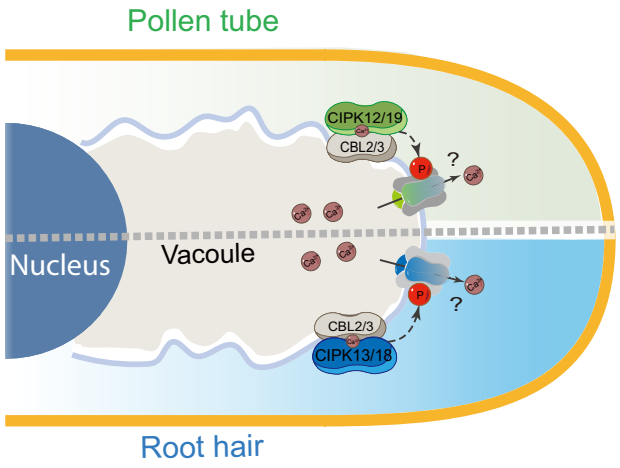

Figure 8. Hypothetical working model of CIPK12/13/18/19 in pollen tube and root hair. The upper and bottom half of the diagram represent pollen tube cell and root hair cell, respectively. CBL-CIPK pairs that decipher Ca^{2+} signals are involved in the polarized cell tip growth in both pollen tube and root hair. In root hair, CIPK13/18 are important while CIPK12/19 act as counterparts in the pollen tube. CBL2/3 are required for both pollen tube and root hair likely by promoting the activity of CIPK12/19 and CIPK13/18 at tonoplast, respectively. The activated CIPK12/13/18/19 phosphorylate downstream substrates such as Ca^{2+} transporters to regulate polarized tip growth. The p in a circle represents potential phosphorylation.

protein kinases, CIPK13/18, are required for root hair growth, establishing a model for further studying the mechanism of Ca^{2+} signaling in polarized cell growth. In parallel, earlier works identified closely related CIPKs, CIPK12/19, as critical regulators of pollen tube growth. Interestingly, in both cases, the same calcium sensors CBL2/3 are involved as upstream regulators of CIPKs. We thus present a working model that CBL-CIPK pairs are involved in polarized cell tip growth of both pollen tube and root hair. In the root hair, CIPK13/18 are important, whereas CIPK12/19 act as counterparts of their homologs in pollen tube. It appears that CBL2/3 recruit different partner CIPKs in pollen tube and root hair to perform downstream cellular functions. Despite difference in CIPKs involved, similar Ca^{2+} decoding mechanism of CBL-CIPK network is adopted in pollen tube and root hair, although these 2 types of cells fulfill completely different physiological roles (Fig. 8).

The findings that the calcium sensors CBL and CIPK are important for the polarized growth in pollen tube and root hair connect well with previous studies identifying a number of Ca^{2+} channels to be essential in the same cell types. For instance, *CNGC18*, encoding a Ca^{2+} influx channel, is exclusively expressed in pollen tube. The removal of *CNGC18* leads to failed pollen tube bugling, premature rapture, and complete fertility (Frietsch et al. 2007). In root hair, *CNGC14* was previously shown to be expressed in root hair cells and contribute to root hair growth. The absence of *CNGC14* causes no obvious defective root hair when grown on the surface of the medium but strikingly shortened root hair

when growing inside of the agar medium (Zhang et al. 2017). Similarly, *cipk13 cipk18* shows dampened root hair growth only when the roots are grown within the agar. We speculate CNGCs function as upstream of CBL-CIPK in mediating polarized growth in pollen tube and root hair. Moreover, calcium signals seem to be regulated through a feedback loop as well. A number of Ca^{2+} channels and transporters are the putative targets of CBL-CIPK complexes. Our results also demonstrated the Ca^{2+} signals and Ca^{2+} oscillations are attenuated in *cipk13/18*, suggesting CIPK13/18 affect intracellular Ca^{2+} abundances and alterations. It is worth investigating whether CNGCs can be directly regulated by CBL-CIPK heterodimers through phosphorylation.

CBL-CIPK modules transduce calcium signals into cellular responses through phosphorylating their substrates. Previous studies revealed a variety of components related to cytoskeleton or vesicle trafficking as central regulators in regulating both pollen tube and root hair (Qi and Greb 2017). In particular, a number of small GTPases are suggested to control cell polarity. Guanine exchange factors (GEFs) and GTPase-activating proteins (GAPs), the activators and repressors of small GTPases, are required for polarized cell growth (Minamino and Ueda 2019; Nielsen 2020; Li et al. 2023). Previous studies have shown that 2 GEF factors for ROPs, RopGEF4 and RopGEF10, function in root hair growth. Like *cipk13 cipk18*, the *gef4 gef10* double mutant displays root hair growth inhibition (Huang et al. 2013). Moreover, 4 CPKs, kinases that act as calcium sensors in addition to CBL-CIPK, interact with and phosphorylate RopGEF1, thereby affecting root hair development (Li et al. 2018). We conjecture that CBL-CIPK and small GTPase function in overlapping signal pathways that are related to Ca^{2+} in modulating root hair growth. It will be interesting to explore whether these GEF components function as directly downstream of CBL2/3-CIPK13/18.

In general, CIPKs are localized at cytosol and can be recruited by partner CBLs to relocate to specific subcellular locations (Luan 2009; Tang et al. 2020). Since CBL2/3 locate at vacuolar membrane, it is implicated that CIPK13/18 target the transmembrane proteins, channels, and transporters that are anchored at tonoplast during polarized cell growth. In addition to calcium, cations and anions, such as potassium (K^+), chloride (Cl^-), and nitrate (NO_3^-), are known to be finely tuned in pollen tube and root hair. For instance, a NO_3^- gradient with oscillations is detected in pollen tube tip (Gutermuth et al. 2013). In addition, SPIK, a K^+ inward channel, helps to maintain a stable cytoplasmic K^+ abundance in pollen tube. Two calcium-activated kinases, CPK11/24, activate SPIK through phosphorylation (Zhao et al. 2013). Moreover, in the absence of MSL8, a mechanosensitive channel functioning in pollen tube, disrupted anion fluxes were detected and reduced pollen tube germination rates were observed (Hamilton et al. 2015). Recent studies also indicated a mechanically sensitive channel that Piezo locates at the vacuolar membrane. Piezo is a putative calcium channel and likely impacts calcium signals (Fang et al. 2021; Mousavi et al. 2021; Radin et al. 2021). Piezo affects vacuolar morphology and pollen tube growth (Radin et al. 2021). Whether the tonoplast-localized channels and transporters for Ca^{2+}, K^+, Cl^-, and NO_3^- are the direct substrates of CBL2/3-CIPK13/18 in root hair awaits further investigations.

Many *cipk* mutant plants analyzed so far merely display relatively subtle defective phenotypes. For instance, *cipk12* and *cipk19* single mutants show mild pollen tube defects. The *cipk12 cipk19* double mutants exhibit no synergic effect. Likewise, we found *cipk13 cipk18* only shows slightly reduced root hair length compared with WT plants. By contrast, the *cngc* mutant plants often exhibit severe defective phenotypes. For instance, the pollen tube growth is completely arrested in *cngc18* and the root hair growth is significantly disrupted in *cngc14*. We postulate that the components that control calcium signal initiation such as calcium channels and transporters are epistatic to downstream Ca^{2+} decoding components including CBLs and CIPKs. Regulators paralleled to CBL-CIPK may fulfill their functions independently. Furthermore, CIPKs appear to be conditionally activated. The *cipk* mutant plants challenged by various stressed stimuli potentially significantly distinguish their phenotypes from those of WT plants.

Materials and methods

Plant materials and growth conditions

Arabidopsis (*A. thaliana*) Col-0 accession was used as WT. The T-DNA insertion alleles *cipk12-3* (CS852223), *cipk13-2* (SALK_124748), *cipk18-1* (SALK_135953), *cipk19-1* (SALK_044735), *cbl1-1* (SALK_110426), *cbl9-1* (SALK_142774), *cbl2-2* (SALK_151426), and *cbl3-2* (SAIL_785_C10) in Col-0 background were obtained from the Arabidopsis Biological Resource Center (ABRC). The *cipk12-c1*, *cipk13-c1*, *cipk18-c1*, *cipk19-c1*, *cbl2-c1*, and *cbl3-c1* mutants in Col-0 background were generated using a CRISPR/Cas9 system from Professor Qijun Chen (Huazhong Agricultural University, China). To construct transgenic plants, the plants were transformed using the *Agrobacterium tumefaciens*-mediated floral dip method (Clough and Bent 1998). Arabidopsis plants were soil grown in a greenhouse under long-day light condition (16-h light/8-h dark per day, light intensity, 22 ± 2 °C). For phenotypic analysis of root hair, surface-sterilized Arabidopsis seeds were placed at 4 °C for 48 h and then germinated on 1/4 MS, 2 mM MES, and 0.8% (w/v) sucrose with 1% (w/v) agar. Plates were placed in a growth chamber at 22 °C with 16-h light/8-h dark condition.

Molecular cloning and construction of transgenic plants

The CDS promoter sequences of *CBLs* and *CIPKs* were PCR amplified (the primer sequences are presented in Supplementary Table S1), and the PCR products were recombined into the *pDONR* vector using the Gateway BP reaction, followed by Gateway LR reaction to construct destination vectors (Invitrogen). For BiFC assay, *CBL* and *CIPK* CDS entries were recombined into the binary vector *pEG202-GWR-nYFP* or *pEG202-GWR-cYFP*. For CIPK expression pattern analysis, the *CIPK* promoter entry vectors were recombined into the binary vector *pBIB-BASTA-GWR-GUS* or *pFYTAG* (Zhang et al. 2005). For constructing overexpression plants, target genes were cloned into the binary vector *pBIB-BASTA-35S-GWR-Flag*. For constructing complementary plants, *CIPK* or *CBL* genome sequences containing promoters and coding sequences with the stop codon were cloned into binary vector *pBIB-BASTA-GWR* or *pGWB16*. The destination vectors were transformed to plants via *A. tumefaciens* strain GV3101 using the floral dip method. T3 generation homozygous transgenic plants were analyzed.

Pollen germination in vitro

The in vitro pollen germination was performed as previously described (Li et al. 1999). In brief, mature pollen grains were dispersed on pollen germination medium in Petri dishes containing 18% (w/v) sucrose, 0.01% (w/v) boric acid, 5 mM $CaCl_2$, 5 mM KCl, 1 mM $MgSO_4$, and 1.5% (w/v) low-melting point agarose, pH 7.5. Petri dishes were then incubated in humid boxes at 22 °C temperature for 4 h. Pollen germination was observed under a microscope (Zeiss Axio Observer Z1). Pollen tube lengths and germination rates were measured using the ImageJ software.

Root hair phenotype analysis

For the analysis of root hairs exposed to air, seeds were sown on the surface of medium in the plates. For the measurement of root hair length, root hairs were covered by a cover glass to push the root hairs down to an angle being parallel to the surface of solid medium for the convenience of root hair phenotype analysis. For the analysis of root hairs embedded in solid medium, seeds were sown on the surface of the solid medium and pushed into the solid medium using a sharp pipette tip. The Petri dishes were placed vertically in a growth room. Pictures were taken under a microscope (Zeiss Axio Observer Z1). The lengths of root hairs were analyzed using the ImageJ software after pictures were taken. Root hairs located within the 2-mm root hair zoom were counted. Time-lapse experiments in bright fields in intact growing roots and hairs were conducted to measure the growth time of root hairs. Four-day-old seedlings grown in a Petri dish were placed vertically in a growth room after seeds were sown on the surface of solid medium. A set of optical sectioning images was captured each 10 min for no less than 60 min at room temperature. For the treatments of plants in different calcium conditions, $CaCl_2$ or EGTA was added to the 1/6 MS, 2 mM MES, and 0.8% (w/v) sucrose with 1% (w/v) agar medium as indicated.

GUS staining

Different tissues of transgenic plants at different developmental stages were collected. Tissues were first incubated in rinse solution (34.2 mM Na_2HPO_4, 15.8 mM NaH_2PO_4, 0.5 mM $K_3Fe(CN)_6$, and 0.5 mM $K_4Fe_6.3H_2O$) for 5 min, then incubated in stain solution (34.2 mM Na_2HPO_4, 15.8 mM NaH_2PO_4, 0.5 mM $K_3Fe(CN)_6$, 0.5 mM $K_4Fe_6.3H_2O$, and 2 mM X-gluc) at 37 °C for appropriate time. After staining, the plant tissues were immersed in 30%, 50%, 75%, and 95% (v/v) ethanol for 1 h and then immersed in 75% (w/v) ethanol. After being decolorized, the tissues were observed with a stereomicroscope (Leica M165 C).

Yeast 2-hybrid assays

The Yeastmaker Transformation System 2 was used according to the manufacturer's manual (Clontech). The interaction tests were performed in yeast (*Saccharomyces cerevisiae*) strain AH109 (Clontech). To identify CIPK-interacting proteins, CIPK coding sequences were cloned into *pGBT9BS* as baits. cDNAs of CBLs were cloned into *pGADGH* as preys. Empty vector combinations were used as negative controls.

Kinase assays

For the phosphorylation assays by using protein blotting, full lengths of *CIPKs* and *CBLs* were PCR amplified and cloned into the *pDEST15* vector with a GST tag (Invitrogen, 11802014) to produce fusion proteins of GST-CIPK13, GST-CIPK18, GST-CBL3, and GST-CBL2. Proteins expressed in *Escherichia coli* were purified with the glutathione agarose beads (Sangon Biotech, C600031) according to the manufacturer's instructions. For phosphorylation assay, 10 μg of each purified fusion protein was incubated in 30 μL kinase buffer (20 mM Tris-HCl, pH 7.5, 2.5 mM $MgCl_2$, 2.5 mM $MnCl_2$, 0.5 mM $CaCl_2$, 100 μM ATP, and 1 mM DTT) for 40 min at 30 °C with gentle shaking. The proteins were then analyzed by immunoblotting with a phospho-threonine/tyrosine antibody (Cell Signaling Technology, 9381).

For in vitro kinase assays, the buffer containing 20 mM Tris-HCl (pH 7.5), 2.5 mM $MnCl_2$, 2.5 mM $MgCl_2$, 1 mM $CaCl_2$, and 1 mM DTT was used. Total volume of 40 μL included 7.5 μCi of [γ-^{32}P]-ATP and the protein combinations indicated in the figure legends. After incubation for 60 min at 30 °C, the reactions were stopped by adding 5× loading buffer. The reactions were resolved on 10% SDS–PAGE, and gels were CBB stained, destained, and dried. The gel was dried, and ^{32}P was detected by autoradiography using a Typhoon 8600 imager (Molecular Dynamics, Piscataway, NJ).

BiFC and subcellular localization assay

For BiFC assay, *A. tumefaciens* strain GV3101 containing vector *CIPK13/18-YN* was mixed with the GV3101 containing *CBL2/3-YC* and infiltrated into the young leaves of *N. benthamiana*. *CBL10* was used as a control. Two days after infiltration, 1.5-cm-diameter infiltrated leaves were incubated with 500 mL protoplast solution containing 500 mM D-mannitol, 10 mM $CaCl_2$, 5 mM MES (pH 5.6), 3% (w/v) Cellulase Onozuka, and 0.75% (w/v) Macerozyme in vacuum for 5 min. The samples were slightly vibrated in the darkness for 4 h. The protoplasts were resuspended with 200 to 500 μL W5 solution (125 mM $CaCl_2$, 5 mM KCl, 154 mM NaCl, 5 mM glucose, and 1.5 mM MES, adjusted pH 5.6 with KOH). PM of leaf mesophyll protoplasts was labeled with FM4-64 and fluorescence signal was detected by a confocal microscope (Leica/Stellaris 5). For YFP visualization, excitation laser at 514 nm and detection between 520 and 550 nm were used (laser intensity at 2% and gain value at 2). For FM4-64 visualization, excitation laser at 561 nm and detection between 570 and 630 nm were used (laser intensity at 3% and gain value at 6). Subcellular localization of CIPK13/18 was determined by detecting the YFP fluorescence signal. The plants were grown on 1/2 MS medium for 5 d. The YFP fluorescence signal was observed by using a laser scanning confocal microscope (Nikon/A1R + Ti2-E). For YFP visualization, excitation laser at 514 nm and detection between 525 and 620 nm were used (laser intensity at 3% and gain value at 1.3). Excitation and emission settings of all samples were kept constant.

Co-IP assay

The full-length cDNAs of *CIPK18* were cloned into *pBIB-Basta-35s-GWR-Flag*, while *CBL3* was fused into *pGWB17* by using Gateway cloning (Invitrogen) and the recombinant plasmids were introduced into *A. tumefaciens* strain GV3101. Different strains were mixed and infiltrated into the leaves of *N. benthamiana*. After 48 h, leaves were harvested and the total protein was extracted by an extraction buffer (50 mM HEPES, 150 mM KCl, 1 mM EDTA, 10% [v/v] glycerol, 0.2% [v/v] Triton X-100, 1 mM DTT, and 2× protease inhibitor cocktail, pH 7.5). The extracted samples were centrifuged by 8,000 × *g* for 30 min at 4 °C. Total protein was dissolved by extraction buffer and incubated with anti-Myc beads (KT-HEALTH, China) for 3 h at 4 °C. Extraction buffer (without Triton X-100) was used to wash the beads 5 times and added 30 μL 2× SDS loading buffer, and then in a water bath at 95 °C for 5 min to obtain the target protein. The samples were subjected to immunoblot analysis by using either anti-Myc (Abmart, China) or anti-Flag antibodies (Abmart, China).

In vivo Ca^{2+} imaging

Transgenic Arabidopsis plants stably expressing *GCaMP6s* were used for in vivo Ca^{2+} imaging as previously described (Shao et al. 2020). In brief, plants were grown on coverslips containing medium for 4 d, and cytoplasmic Ca^{2+} imaging of root hair was obtained using a spinning disk confocal microscope equipped with an iXON ultra EMCCD camera (Andor). Image acquisition was performed using the Andor IQ3 software. GFP was excited with a 488-nm laser and observed using a 514-nm emission filter. Images were quantified with the ImageJ software. This experiment was made for 4 biological replicates with similar results.

Data acquisition and statistics

All experiments were repeated at least 3 times. The statistical analyses were indicated in each figure legend and were performed using the program GraphPad Prism v8. Statistical significance is indicated by the *P* value, $P < 0.05$, marked with different characters.

Accession numbers

Sequence data from this article can be found in the GenBank/EMBL data libraries under accession numbers CIPK13 (NM_128969), CIPK18 (NM_102663), CBL2 (NM_124981), and CBL3 (NM_118791). Sequence data from this article can be found in the Arabidopsis Information Resource database (TAIR, http://www.arabidopsis.org/) under the following accession numbers: *CIPK13*, *AT2G34180*; *CIPK18*, *AT1G29230*; *CBL2*, *AT5G55990*; and *CBL2*, *AT4G26570*.

Acknowledgments

We thank Liang Peng, Liping Guan, Yahu Gao, Yang Zhao, and Li Xie (Core Facility for Life Science Research, Lanzhou University) for technical support.

Author contributions

K.H., X.F., and S.L. conceived the project and designed the experiments. K.H., X.F., and S.L. wrote the manuscript. X.F. and B.L. performed most of the experiments. H.K., J.Z., Y.F., C.X., Q.S., X.H., and Y.W. performed the others. A.B. and J.L. helped prepare the manuscript.

Supplementary data

The following materials are available in the online version of this article.

Supplementary Figure S1. Identification of *cipk* T-DNA insertion mutants.

Supplementary Figure S2. *CIPK12* and *CIPK19* are required for pollen tube growth.

Supplementary Figure S3. *CIPK13 and CIPK18* are not required for pollen tube growth.

Supplementary Figure S4. Expression patterns of *CIPK12/13/18/19*.

Supplementary Figure S5. Expression of *CIPK12/19* and *CIPK13/18* in pollen and pollen tube.

Supplementary Figure S6. *cipk13 cipk18* shows no obvious root hair defects when the roots are grown on the surface of the medium.

Supplementary Figure S7. Construction of *cipk12-c1*, *cipk13-c1*, *cipk18-c1*, and *cipk19-c1* by using CRISPR/Cas9.

Supplementary Figure S8. Identification of the mutant plants.

Supplementary Figure S9. *CIPK12* and *CIPK19* are not required for root hair growth.

Supplementary Figure S10. The root hair phenotypes of *cipk13-2 cipk18-1* under different calcium conditions.

Supplementary Figure S11. The root hair phenotype of *cbl2 cbl3*.

Supplementary Figure S12. CIPK13/18 are not activated by GST.

Supplementary Figure S13. OSCA2.3 loop interacts with CIPK18.

Supplementary Table S1. Primer sequences used in this study.

Supplementary Video S1. Calcium oscillations in *cipk13 cipk18* root hair.

Funding

This work was supported by the National Natural Science Foundation of China (32370295 and 32170280 to K.H., 32200232 to Y.W.), the Science and Technology Department of Gansu Province (23JRRA1138 to X.F., 23JRRA1132 to C.X.), and the U.S. National Science Foundation (MCB-2041585 to S.L.).

Conflict of interest statement. The authors declare that they have no conflict of interest with this work.

Data availability

All data that support the findings of this study are available in the main paper and Supplemental data.

References

Bibikova TN, Zhigilei A, Gilroy S. Root hair growth in *Arabidopsis thaliana* is directed by calcium and an endogenous polarity. *Planta*. 1997:203(4):495–505. https://doi.org/10.1007/s004250050219

Brost C, Studtrucker T, Reimann R, Denninger P, Czekalla J, Krebs M, Fabry B, Schumacher K, Grossmann G, Dietrich P. Multiple cyclic nucleotide-gated channels coordinate calcium oscillations and polar growth of root hairs. *Plant J*. 2019:99(5):910–923. https://doi.org/10.1111/tpj.14371

Clough SJ, Bent AF. Floral dip: a simplified method for Agrobacterium-mediated transformation of *Arabidopsis thaliana*. *Plant J*. 1998:16(6):735–743. https://doi.org/10.1046/j.1365-313x.1998.00343.x

Cole RA, Fowler JE. Polarized growth: maintaining focus on the tip. *Curr Opin Plant Biol*. 2006:9(6):579–588. https://doi.org/10.1016/j.pbi.2006.09.014

Creamer TP. Calcineurin. *Cell Commun Signal*. 2020:18(1):137. https://doi.org/10.1186/s12964-020-00636-4

Dodd AN, Kudla J, Sanders D. The language of calcium signaling. *Annu Rev Plant Biol*. 2010:61(1):593–620. https://doi.org/10.1146/annurev-arplant-070109-104628

Duszyn M, Swiezawska B, Szmidt-Jaworska A, Jaworski K. Cyclic nucleotide gated channels (CNGCs) in plant signalling—current knowledge and perspectives. *J Plant Physiol*. 2019:241:153035. https://doi.org/10.1016/j.jplph.2019.153035

Edel KH, Marchadier E, Brownlee C, Kudla J, Hetherington AM. The evolution of calcium-based signalling in plants. *Curr Biol*. 2017:27-(13):R667–R679. https://doi.org/10.1016/j.cub.2017.05.020

Fang X, Liu B, Shao Q, Huang X, Li J, Luan S, He K. AtPiezo plays an important role in root cap mechanotransduction. *Int J Mol Sci*. 2021:22(1):467. https://doi.org/10.3390/ijms22010467

Frietsch S, Wang YF, Sladek C, Poulsen LR, Romanowsky SM, Schroeder JI, Harper JF. A cyclic nucleotide-gated channel is essential for polarized tip growth of pollen. *Proc Natl Acad Sci U S A*. 2007:104(36):14531–14536. https://doi.org/10.1073/pnas.0701781104

Gutermuth T, Lassig R, Portes MT, Maierhofer T, Romeis T, Borst JW, Hedrich R, Feijo JA, Konrad KR. Pollen tube growth regulation by free anions depends on the interaction between the anion channel SLAH3 and calcium-dependent protein kinases CPK2 and CPK20. *Plant Cell*. 2013:25(11):4525–4543. https://doi.org/10.1105/tpc.113.118463

Hamilton ES, Jensen GS, Maksaev G, Katims A, Sherp AM, Haswell ES. Mechanosensitive channel MSL8 regulates osmotic forces during pollen hydration and germination. *Science*. 2015:350(6259):438–441. https://doi.org/10.1126/science.aac6014

Harper JE, Breton G, Harmon A. Decoding Ca^{2+} signals through plant protein kinases. *Annu Rev Plant Biol*. 2004:55(1):263–288. https://doi.org/10.1146/annurev.arplant.55.031903.141627

Hepler PK, Vidali L, Cheung AY. Polarized cell growth in higher plants. *Annu Rev Cell Dev Biol*. 2001:17(1):159–187. https://doi.org/10.1146/annurev.cellbio.17.1.159

Hetherington AM, Brownlee C. The generation of Ca^{2+} signals in plants. *Annu Rev Plant Biol*. 2004:55(1):401–427. https://doi.org/10.1146/annurev.arplant.55.031903.141624

HoldawayClarke TL, Feijo JA, Hackett GR, Kunkel JG, Hepler PK. Pollen tube growth and the intracellular cytosolic calcium gradient oscillate in phase while extracellular calcium influx is delayed. *Plant Cell*. 1997:9(11):1999–2010. https://doi.org/10.2307/3870560

Huang GQ, Li E, Ge FR, Li S, Wang Q, Zhang CQ, Zhang Y. Arabidopsis RopGEF4 and RopGEF10 are important for FERONIA-mediated developmental but not environmental regulation of root hair growth. *New Phytol*. 2013:200(4):1089–1101. https://doi.org/10.1111/nph.12432

Hussey PJ, Ketelaar T, Deeks MJ. Control of the actin cytoskeleton in plant cell growth. *Annu Rev Plant Biol*. 2006:57(1):109–125. https://doi.org/10.1146/annurev.arplant.57.032905.105206

Kropf DL, Bisgrove SR, Hable WE. Cytoskeletal control of polar growth in plant cells. *Curr Opin Cell Biol*. 1998:10(1):117–122. https://doi.org/10.1016/S0955-0674(98)80094-X

Kudla J, Batistic O, Hashimoto K. Calcium signals: the lead currency of plant information processing. *Plant Cell*. 2010:22(3):541–563. https://doi.org/10.1105/tpc.109.072686

Li E, Zhang YL, Qin Z, Xu M, Qiao Q, Li S, Li SW, Zhang Y. Signaling network controlling ROP-mediated tip growth in Arabidopsis and beyond. *Plant Commun*. 2023:4(1):100451. https://doi.org/10.1016/j.xplc.2022.100451

Li H, Lin Y, Heath RM, Zhu MX, Yang Z. Control of pollen tube tip growth by a Rop GTPase-dependent pathway that leads to tip-localized calcium influx. *Plant Cell*. 1999:11(9):1731–1742. https://doi.org/10.1105/tpc.11.9.1731

Li Z, Takahashi Y, Scavo A, Brandt B, Nguyen D, Rieu P, Schroeder JI. Abscisic acid-induced degradation of Arabidopsis guanine nucleotide exchange factor requires calcium-dependent protein kinases. *Proc Natl Acad Sci U S A*. 2018:115(19):E4522–E4531. https://doi.org/10.1073/pnas.1719659115

Luan S. The CBL-CIPK network in plant calcium signaling. *Trends Plant Sci*. 2009:14(1):37–42. https://doi.org/10.1016/j.tplants.2008.10.005

Luan S, Wang C. Calcium signaling mechanisms across kingdoms. *Annu Rev Cell Dev Biol*. 2021:37(1):311–340. https://doi.org/10.1146/annurev-cellbio-120219-035210

McAinsh MR, Pittman JK. Shaping the calcium signature. *New Phytol*. 2009:181(2):275–294. https://doi.org/10.1111/j.1469-8137.2008.02682.x

Minamino N, Ueda T. RAB GTPases and their effectors in plant endosomal transport. *Curr Opin Plant Biol*. 2019:52:61–68. https://doi.org/10.1016/j.pbi.2019.07.007

Mousavi SAR, Dubin AE, Zeng WZ, Coombs AM, Do K, Ghadiri DA, Keenan WT, Ge C, Zhao Y, Patapoutian A. PIEZO ion channel is required for root mechanotransduction in *Arabidopsis thaliana*. *Proc Natl Acad Sci U S A*. 2021:118(20):e2102188118. https://doi.org/10.1073/pnas.2102188118

Nielsen E. The small GTPase superfamily in plants: a conserved regulatory module with novel functions. *Annu Rev Plant Biol*. 2020:71(1):247–272. https://doi.org/10.1146/annurev-arplant-112619-025827

Pacheco JM, Gabarain VB, Lopez LE, Lehuede TU, Ocaranza D, Estevez JM. Understanding signaling pathways governing the polar development of root hairs in low-temperature, nutrient-deficient environments. *Curr Opin Plant Biol*. 2023:75:102386. https://doi.org/10.1016/j.pbi.2023.102386

Pan Y, Chai X, Gao Q, Zhou L, Zhang S, Li L, Luan S. Dynamic interactions of plant CNGC subunits and calmodulins drive oscillatory Ca^{2+} channel activities. *Dev Cell*. 2019:48(5):710–725.e715. https://doi.org/10.1016/j.devcel.2018.12.025

Qi J, Greb T. Cell polarity in plants: the Yin and Yang of cellular functions. *Curr Opin Plant Biol*. 2017:35:105–110. https://doi.org/10.1016/j.pbi.2016.11.015

Radin I, Richardson RA, Coomey JH, Weiner ER, Bascom CS, Li T, Bezanilla M, Haswell ES. Plant PIEZO homologs modulate vacuole morphology during tip growth. *Science*. 2021:373(6554):586–590. https://doi.org/10.1126/science.abe6310

Rounds CM, Bezanilla M. Growth mechanisms in tip-growing plant cells. *Annu Rev Plant Biol*. 2013:64(1):243–265. https://doi.org/10.1146/annurev-arplant-050312-120150

Shao QL, Gao QF, Lhamo D, Zhang HS, Luan S. Two glutamate- and pH-regulated Ca^{2+} channels are required for systemic wound signaling in. *Sci Signal*. 2020:13(640):eaba145. https://doi.org/10.1126/scisignal.aba1453

Steinhorst L, Mahs A, Ischebeck T, Zhang C, Zhang X, Arendt S, Schultke S, Heilmann I, Kudla J. Vacuolar CBL-CIPK12 Ca^{2+}-sensor-kinase complexes are required for polarized pollen tube growth. *Curr Biol*. 2015:25(11):1475–1482. https://doi.org/10.1016/j.cub.2015.03.053

Sugiura R, Sio SO, Shuntoh H, Kuno T. Calcineurin phosphatase in signal transduction: lessons from fission yeast. *Genes Cells*. 2002:7(7):619–627. https://doi.org/10.1046/j.1365-2443.2002.00557.x

Tan YQ, Yang Y, Zhang A, Fei CF, Gu LL, Sun SJ, Xu W, Wang L, Liu H, Wang YF. Three CNGC family members, CNGC5, CNGC6, and CNGC9, are required for constitutive growth of Arabidopsis root hairs as Ca^{2+}-permeable channels. *Plant Commun*. 2020:1(1):100001. https://doi.org/10.1016/j.xplc.2019.100001

Tang RJ, Liu H, Yang Y, Yang L, Gao XS, Garcia VJ, Luan S, Zhang HX. Tonoplast calcium sensors CBL2 and CBL3 control plant growth and ion homeostasis through regulating V-ATPase activity in Arabidopsis. *Cell Res*. 2012:22(12):1650–1665. https://doi.org/10.1038/cr.2012.161

Tang RJ, Wang C, Li KL, Luan S. The CBL-CIPK calcium signaling network: unified paradigm from 20 years of discoveries. *Trends Plant Sci*. 2020:25(6):604–617. https://doi.org/10.1016/j.tplants.2020.01.009

Tian W, Wang C, Gao Q, Li L, Luan S. Calcium spikes, waves and oscillations in plant development and biotic interactions. *Nat Plants*. 2020:6(7):750–759. https://doi.org/10.1038/s41477-020-0667-6

Weinl S, Kudla J. The CBL-CIPK Ca^{2+}-decoding signaling network: function and perspectives. *New Phytol*. 2009:184(3):517–528. https://doi.org/10.1111/j.1469-8137.2009.02938.x

Zhang CQ, Gong FC, Lambert GM, Galbraith DW. Cell type-specific characterization of nuclear DNA contents within complex tissues and organs. *Plant Methods*. 2005:1(1):7. https://doi.org/10.1186/1746-4811-1-7

Zhang R, Xu Y, Yi R, Shen J, Huang S. Actin cytoskeleton in the control of vesicle transport, cytoplasmic organization and pollen tube tip growth. *Plant Physiol*. 2023:193(1):9–25. https://doi.org/10.1093/plphys/kiad203

Zhang S, Pan Y, Tian W, Dong M, Zhu H, Luan S, Li L. Arabidopsis CNGC14 mediates calcium influx required for tip growth in root hairs. *Mol Plant*. 2017:10(7):1004–1006. https://doi.org/10.1016/j.molp.2017.02.007

Zhao LN, Shen LK, Zhang WZ, Zhang W, Wang Y, Wu WH. Ca^{2+}-dependent protein Kinase11 and 24 modulate the activity of the inward rectifying K^+ channels in Arabidopsis pollen tubes. *Plant Cell*. 2013:25(2):649–661. https://doi.org/10.1105/tpc.112.103184

Zhou L, Lan W, Chen B, Fang W, Luan S. A calcium sensor-regulated protein kinase, CALCINEURIN B-LIKE PROTEIN-INTERACTING PROTEIN KINASE19, is required for pollen tube growth and polarity. *Plant Physiol*. 2015:167(4):1351–1360. https://doi.org/10.1104/pp.114.256065